Initiator Addition to Methyl Methacrylate Studied in Liquid and Supercritical Carbon Dioxide

Malcolm D. E. Forbes* and Haruhiko Yashiro

Caudill Laboratories, Department of Chemistry, CB# 3290, University of North Carolina, Chapel Hill, North Carolina 27599

Received October 22, 2006; Revised Manuscript Received December 10, 2006

ABSTRACT: The photochemistry and radical chemistry of two widely used photoinitiators have been studied in liquid and supercritical carbon dioxide solutions and compared to conventional solvents such as acetonitrile and toluene. A specially modified time-resolved electron paramagnetic resonance (TREPR) apparatus was used to detect free radicals produced from the triplet states of dimethoxyphenylacetophenone (DMPA, **1**) and trimethylbenzoyldiphenylphosphine oxide (TMDPO, **2**) after excitation of the parent compounds using a 308 nm excimer laser. The photochemistry and photophysics of these molecules in CO_2 are similar to those observed in conventional solvents. In the presence of methyl methacrylate (MMA) monomer, both benzoyl (**1a**) and dimethoxybenzyl (**1b**) radicals from DMPA react to form adduct radicals **1c** and **1d**, which are indistinguishable by TREPR. The MMA concentration dependence and time dependence of these spectra are simulated and discussed. From **2**, the trimethylbenzoyl radical **2a** is much less reactive than the diphenylphosphinyl oxide radical **2b**. Measurement of the TREPR line width at a constant delay time as a function of MMA concentration gives the rate of addition, k_{add}, of **2b** to MMA ($(5.5 \pm 0.5) \times 10^7$ M^{-1} s^{-1} in liquid CO_2; $(6.1 \pm 0.6) \times 10^7$ M^{-1} s^{-1} in supercritical CO_2). These values are close to those observed in acetonitrile ($(8.1 \pm 1.6) \times 10^7$ M^{-1} s^{-1}) and toluene ($(4.0 \pm 0.4) \times 10^7$ M^{-1} s^{-1}).

Introduction

The addition of a free radical to an alkene is ubiquitous in polymer synthesis, where it finds application in the emulsion, dispersion, and homogeneous polymerizations of many reactive monomers.[1] Over the past 15 years these reactions have been successfully carried out using liquid or supercritical carbon dioxide as the solvent.[2] The "green" chemistry surrounding CO_2 as a reaction medium has led to major advances in the synthetic methodology of polymers,[3] in nanotechnology,[4,5] and in lowering the cost of production of several economically important macromolecules.[6] In almost all of these advances, free radical initiation, propagation, and termination reactions are used, often in conjunction with suitable stabilizers[7] and tunable solvent properties,[8] to optimize desirable features of the polymer products.

Our research group has been interested for some time in the structure, dynamics, and reactivity of free radicals in this unusual solvent. In 1997 we reported the construction of a fast, 9.5 GHz time-resolved electron paramagnetic resonance (TREPR) spectrometer for such studies.[9] We have used this apparatus to investigate radical structures and dynamic processes in both liquid and supercritical CO_2, including (1) the initiation process itself, especially those relevant to synthesis of CO_2-philic polymers,[10] (2) how chain dynamics influence the spin exchange interaction in flexible polymethylene chain biradicals,[11] and (3) an unusual and previously unobserved electron spin relaxation phenomenon for flexible biradicals.[12] In all of our previous studies it has proven useful to compare our observed TREPR spectra to conventional solvents as this has often helped to understand changes in the spectra, which can be subtle.

In this paper we turn our attention to the addition reaction of a free radical to an alkene in CO_2, with an emphasis on the study of typical polymer photoinitiators in the presence of methyl methacrylate (MMA). The two initiators used in this work are shown in Scheme 1, along with the photochemistry leading to free radicals and the MMA adduct radicals from the initiator addition reaction. The photochemistry of these compounds[13] and the physical properties of the ensuing radicals[14−16] have been extensively studied in conventional solvents and are well understood. In a previous study by Jent et al.,[17] two-photon processes have been observed in **1** that lead to the production of methyl radicals and methyl benzoate, but for the low light fluxes used in our experiments we do not need to be concerned with such processes. Of all the radicals depicted in Scheme 1, the diphenylphospinoxyl structure **2b** is likely to be the most reactive (it is the most electron-deficient radical center), followed by **1b**. Of the much less reactive benzoyl structures we expect to see less reactivity from the more sterically hindered trimethyl benzoyl radical **2a**.

Many researchers have studied propagation rates for MMA and other common alkene monomers.[18−20] Because of the unique solvent properties of CO_2 and the growing utility of this solvent for environmentally benign industrial polymerization processes, measurement of the initiator addition rate (k_{add}) in this unusual medium is of considerable interest. The value of k_{add} can be determined by measuring the decay of the transient absorption peaks of the radicals[21] or by examining the TREPR line width at a constant delay time.[22] In general, relating changes in TREPR spectral intensities to chemical lifetimes requires careful measurement and independent confirmation of several system-dependent parameters such as the electron spin relaxation times and EPR microwave cavity resonator properties. Although k_{add} values have been reported previously from such measurements,[21] these important experimental parameters were not determined in that work. An additional complication regarding quantification of TREPR intensities is the presence of chemically induced electron spin polarization (CIDEP) in the spectra.[23] The decay of this polarization in liquid solutions is typically through electron spin relaxation mechanisms. Even with fast chemical

* Corresponding author. E-mail: mdef@unc.edu.

10.1021/ma062438a CCC: $37.00
Published on Web 01/23/2007

Scheme 1

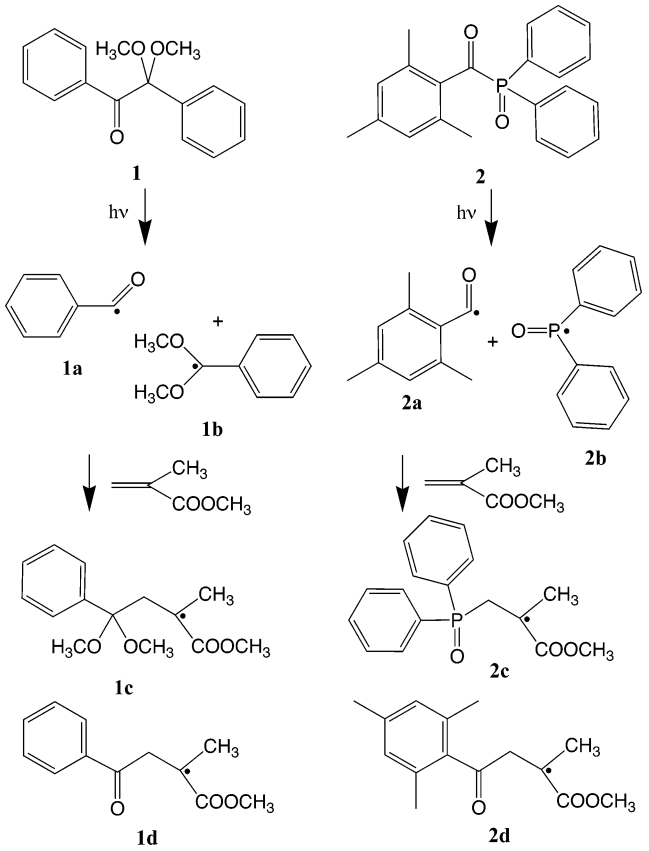

reaction rates, the T_1 values of all the radicals present in any given system should be known independently if accurate determination of the reaction rate is desired.[24]

The line width method mentioned above is independent of spectrometer parameters and polarization effects if radical concentrations are low, and the measurements are made at exactly the same delay time after the laser flash. We employ the method here to extract the k_{add} value for DPP/MMA in four solvents, including liquid and supercritical CO_2. To the best of our knowledge, no measurements of k_{add} have been reported for any initiator or monomer in CO_2.

Experimental Section

Materials. Both initiators were purchased from Aldrich and used without further purification. Methyl methacrylate (Aldrich) was dried over calcium chloride and distilled immediately prior to all experiments.

TREPR Spectroscopy in CO_2. Our TREPR apparatus has been described in detail previously,[25] and our modifications for high pressure are detailed in a separate publication.[9] Briefly, spectra were recorded on a Varian E-line X-band (9.5 GHz) EPR console and bridge modified with a fast preamplifier and a low noise GaAs FET microwave amplifier (25 dB gain). The microwave power incident on the samples was 10 mW for all experiments. High-pressure CO_2 solutions were circulated through a quartz flow cell of 9 mm outside diameter and 2 mm inside diameter using a specially modified Micropump with a sapphire shaft. The quartz sample tube was epoxied to stainless steel pressurizing heads and centered in a home-built brass cylindrical TE_{011} microwave cavity equipped with a slotted window for light access. The flow system is routinely pressure-tested to 200 bar, and experiments are then run below 180 bar. The solutions were irradiated by a 308 nm laser pulse (20 ns width, ~10 mJ hitting the sample, repetition rate 60 Hz) from a XeCl excimer laser LPX100i (Lambda Physik). Spectra were collected at a fixed delay time after the laser flash using a Stanford Research Systems boxcar integrator (100 ns gates), and the external field was swept over 2 or 4 min. For consistency, the experiments in toluene were run using the same apparatus and flow cell. A smaller inner diameter flow cell was used for experiments for more polar solvents (acetonitrile and ethanol).

Safety Note. On occasion, when ramping up the pressure we have experienced the shattering of sample cells or failure of the epoxy seals between the quartz tube and the stainless steel pressurizing heads. Initial pressurization of such flow systems should always be carried out with full face protection. We also recommend using a plexiglass safety shield around the sample cell/resonator assembly at all times when the pressure is above ambient.

Results and Discussion

Figure 1 shows TREPR spectra and simulations for radicals detected after laser flash photolysis at 308 nm of **1** in supercritical CO_2. In Figure 1A only compound **1** is present, and the expected free radicals are **1a** and **1b**, confirmed by the simulation in Figure 1B using spectral parameters listed in the figure caption. The signal from benzoyl radical **1a** is not very intense and manifests itself only as an additional intensity and line width slightly downfield from the signal assigned to radical **1b**. The low intensity of the **1a** signal is due to fast spin relaxation, a common feature in the TREPR spectroscopy of acyl radicals.[26,27] This relaxation process has been extensively investigated by several researchers and, specifically for this benzoyl radical,[28] is due to a large spin−rotation interaction. The parameters used for the simulation of dimethoxybenzyl radical **1b** are consistent with literature values,[17] indicating that radical structures are not strongly perturbed under supercritical solvent conditions.

Figure 1C shows the same system in a slightly lower pressure but still supercritical CO_2 solution with 6.0 M MMA monomer added. This spectrum was acquired at 0.5 μs after the laser flash. An arrow indicates the presence of new peaks on the shoulder of the signal due to **1b** along with other peaks on the perimeter. We assign these new peaks to the adduct radicals **1c** and **1c**, arising from attack of MMA by **1a** and **1b**, respectively. Since there are no hyperfine couplings adjacent to the attacking radical center in either **1a** or **1b**, both adduct radicals have essentially identical spectra. For this reason it is not possible to state which of **1c** or **1d** is present in higher concentration. Simulation of this spectrum is shown in Figure 1D, with the parameters listed in the figure caption. These parameters agree well with those reported by Karatekin[29] and Mizuta[30] for both radicals. The high degree of overlap of the transitions between **1b** and **1c**/**1d** is somewhat problematic in making these fits, as is the signal-to-noise ratio. However, they are satisfactory for the present purpose of radical identification. The relative reactivity of **1a** and **1b** as related to the spectral analysis of Figure 1C,D will be discussed in more detail below.

Figure 1E shows the TREPR spectrum obtained for the same system as in Figure 1C, except that the data were collected at a later delay time, 2.0 μs. This spectrum has been scaled up to show detail. It is clear by inspection and from the simulation in Figure 1F that the adduct radical is now present in a higher concentration (**1c**/**1d**:**1b** = 3:2 here vs 1:2 in Figure 1C). Because of the overlapping lines from the different signal carriers, is difficult to tell whether the line width of **1b** has changed from 0.5 to 2.0 μs. By visual comparison of the spectra in Figure 1C,E it can be stated with certainty that any changes in this line width must be minor.

The dominant spin polarization mechanism in these spectra is the TM, which shows net emission as expected for an acetophenone derivative. There is a small amount of RPM

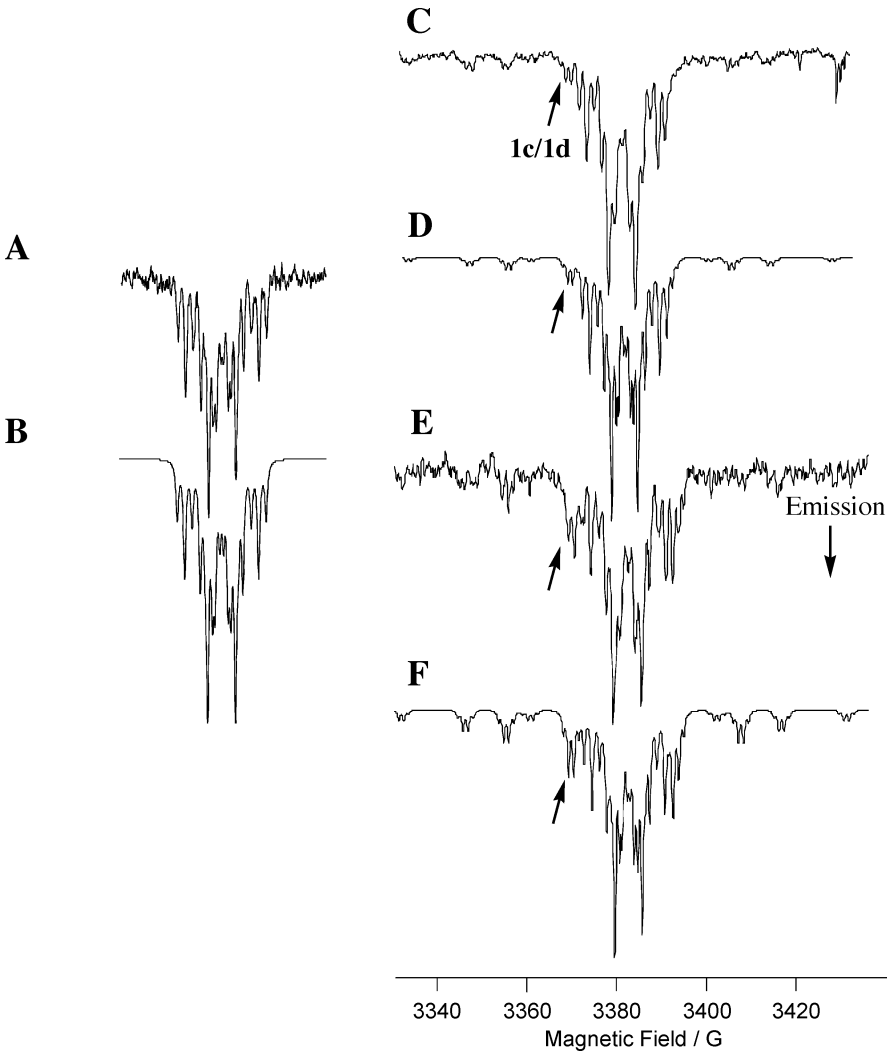

Figure 1. (A) X-band TREPR spectrum acquired in supercritical CO_2 (319 K, 120 bar) 0.5 μs after 308 nm photoexcitation of 0.01 M DMPA (**1**). (B) Simulation using the following parameters for radical **1b**: hyperfine coupling constants: 14.83 G (ortho, 2H), 5.80 G (para, 1H), and 1.65 G (meta, 2H); $g = 2.0028$; line width (full width at half-maximum) = 0.6 G. For radical **1a**, $g = 2.0006$ and line width = 2.0 G. (C) TREPR spectrum acquired using 0.01 M DMPA and 6.0 M methyl methacrylate in supercritical CO_2 (306 K, 75 bar) taken at 0.5 μs after the laser flash. The vertical scale is 5 time larger than the scale in (A). (D) Simulation of the spectrum in (C) using the hyperfine coupling constants listed above for radical **1b**. For the adduct radical **1d** hyperfine coupling constants were 13.7 G (β-CH_2), 22.3 G (β-CH_3), 1.1 G ($-OCH_3$), g-factor = 2.0031, and line width = 0.6 G. (E) Same conditions as (C) except the spectrum was acquired at a delay time of 2.0 μs. (F) Simulation of (E) using the same parameters listed above for both radicals. In (D) the ratio of integrated intensities of **1b** to **1d** in the simulation is 2:1, and in (F) this ratio is 2:3.

polarization superimposed on the spectrum, which has an E/A CIDEP pattern expected from a triplet precursor excited state and a negative exchange interaction in the radical pair. The RPM polarization is only clearly observable in Figure 1A as a slight difference in intensities between the two most intense high and low field transitions. It is not included in the simulation in Figure 1B because the simulation is only used to confirm the identity of the radical from line positions. The coarse intensities are approximately equal to the calculated binomial coefficients for each transition.

It is interesting to note the large concentration of MMA required to see significant signals from the adduct radical(s). This observation, along with the relatively small change in line width of **1b** at 2.0 μs, suggests that the reaction rate of either **1a** or **1b** with MMA is quite slow ($<10^5$ M^{-1} s^{-1}) compared to other initiators. Because of the spectral overlap between the two radicals, it is not possible to quantify this reaction rate further. As mentioned above, analysis of the intensities is complicated by the fact that both radicals are undergoing spin relaxation of their chemically induced spin polarization. It is fair to say that Figure 1 highlights more of the disadvantages one can encounter in such experiments rather than advantages, but the results are nonetheless qualitatively informative regarding k_{add} and quantitative regarding the radical structures.

Photoinitiator **2** is more promising for the extraction of rate information because of the large hyperfine splitting expected from phosphorus-centered radical **2b**. This is expected to lead to very well-resolved, isolated transitions from which precise line widths can be extracted. Figure 2A shows the TREPR spectrum obtained in ethanol solution 0.4 μs after 308 nm excitation of **2**. Here we see only three transitions: a broad singlet at $g = 2.0006$ from the trimethylbenzoyl radical **2a** and a doublet from the phosphinyl radical **2b** at $g = 2.0035$, ^{31}P hyperfine splitting $\sim$ 380 G. Photoexcitation of **2** in liquid CO_2 leads to exactly the same spectrum (not shown). Addition of 0.19 M MMA to this system in CO_2, with observation at a delay time of 0.1 μs, leads to the spectrum shown in Figure 2B. In comparison with Figure 2A, three notable new features are observed: (1) There is a substantial decrease in the intensity of the signal from **2b** relative to **2a**, which is unlikely to be due to spin relaxation because the spectrum is acquired at an *earlier* delay time than in Figure 2A. Makarov et al. have measured T_1

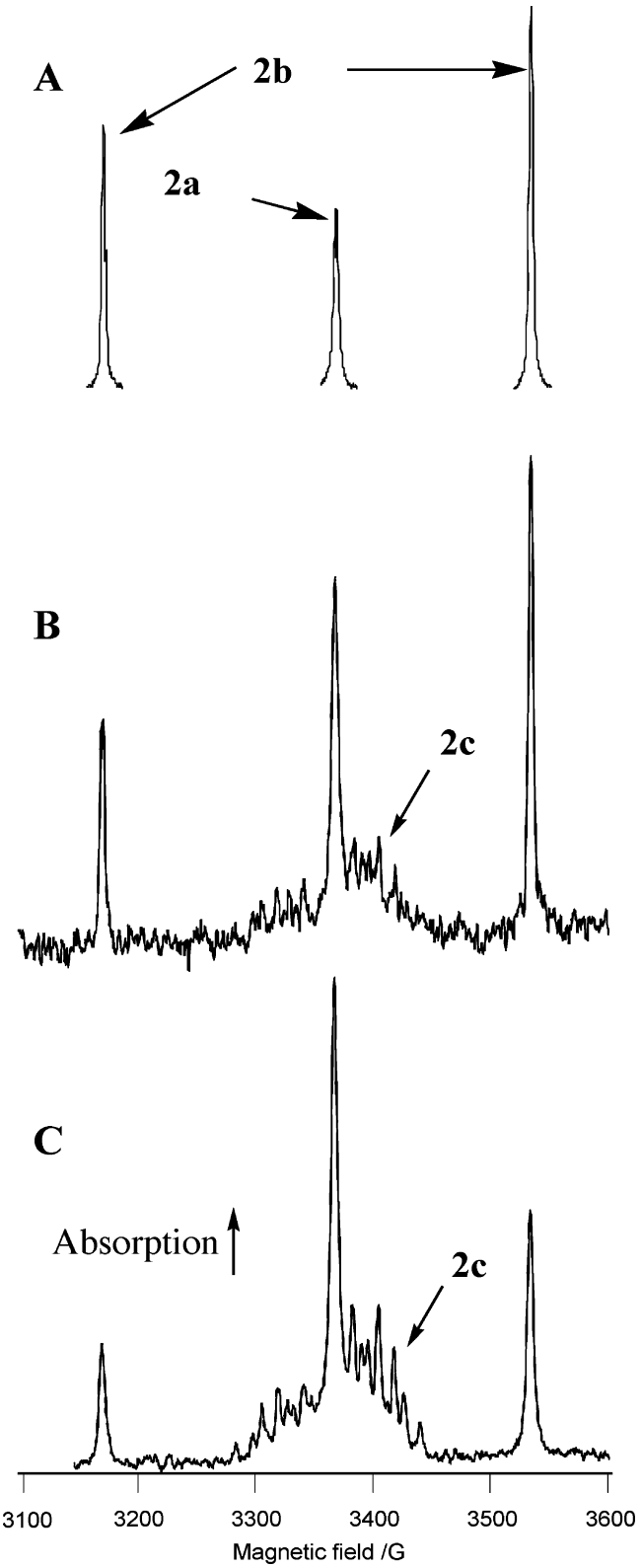

Figure 2. (A) X-band TREPR spectrum acquired in ethanol 0.4 μs after 308 nm photoexcitation of 0.01 M TMDPO (**2**) at 295 K. (B) TREPR spectrum acquired in liquid CO_2 (295 K, 172 bar) 0.1 μs after photolysis of 0.01 M **2** and 0.19 M MMA. (C) Same as (B) except [MMA] = 0.38 M. Microwave power was 1 mW in all spectra.

for radical **2b** to be 600 ns,[31] and these spectra were acquired well within that time frame. (2) There is a new signal carrier in the center of the spectrum, which we assign to the adduct radical **2c**. (3) The polarization mechanism, while still predominantly due to the TM, is now net absorptive rather than emissive, and

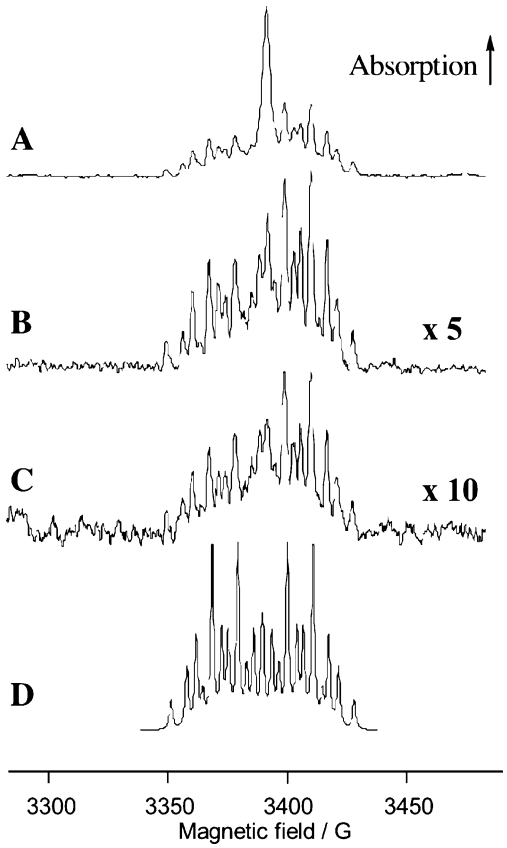

Figure 3. Time dependence of the X-band TREPR spectra obtained under the same conditions as in Figure 2C (0.01 M **2**, 0.38 M MMA, liquid CO_2). These spectra are expanded on the *x*-axis to show the hyperfine splittings in the adduct radical **2c**. Delay times are (A) 0.1 μs, (B) 0.5 μs (scaled up $\times$ 5), and (C) 1.0 μs (scaled up $\times$ 10). (D) Simulation of radical **2c** at 0.5 μs using hyperfine couplings constants of 13.5 G (β-CH_2), 21.6 G (β-CH_3), and 63.8 G (^{31}P); $g = 2.0035$, line width = 3.0 G.

the RPM polarization, while still E/A in phase, is higher in intensity than in Figure 1.

Figure 2C shows the TREPR spectrum acquired 0.1 μs after 308 nm excitation of **2** in liquid CO_2 with 0.38 M MMA. Doubling the concentration of MMA leads to an increase in the signal due to adduct radical **2c**, and again there is a notable decrease in the signal from **2b** relative to **2a**. Clearly the phosphonyl radical **2b** is much more reactive than the trimethylbenzoyl radical **2a**, and this leads us to assign the adduct radical **2c** to a single structure, as shown in Scheme 1. There is no evidence any major reactivity of **2a** to give the other adduct radical **2d**. The observed net A from the TM is expected for radicals from precursors such as **2**, and the increase in the magnitude of the RPM polarization in this system is due to the larger hyperfine coupling of the phosphorus-centered radical.

The time dependence of the TREPR spectra from photolysis of **2** is shown in Figure 3 on an expanded *x*-axis scale so that the hyperfine structure of the adduct radical can be clearly seen. Here the transitions due to radical **2c** are off-scale and not displayed. The delay times shown in parts A, B, and C of Figure 3 are 0.1, 0.5, and 1.0 μs, respectively. The decrease in signal intensity of radical **2a** is most likely due to spin relaxation, and it is interesting to note that this process is much slower for the substituted trimethylbenzoyl structure **2a** than for the parent benzoyl radical **1a**. The relaxation mechanism is from spin rotation interaction in the acyl moiety, and the ortho-methyl groups in **2a** clearly have a strong effect on this motion. Figure 3D shows a simulation of the adduct radical **2c**, optimized to

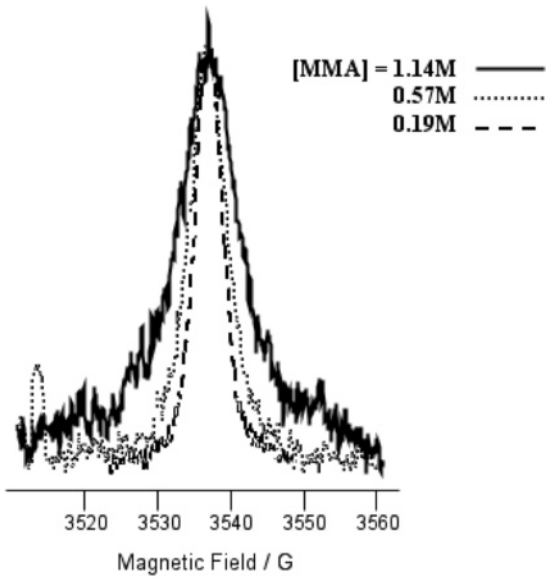

Figure 4. (A) TREPR spectrum from Figure 3A scaled up × 10 to show residual peaks from phosphonyl radical **2b** on the perimeter, indicated by arrows. (B) High field TREPR line of radical **2b**, signal averaged, shown for three different concentrations of MMA. Lines are normalized so that widths can be compared directly.

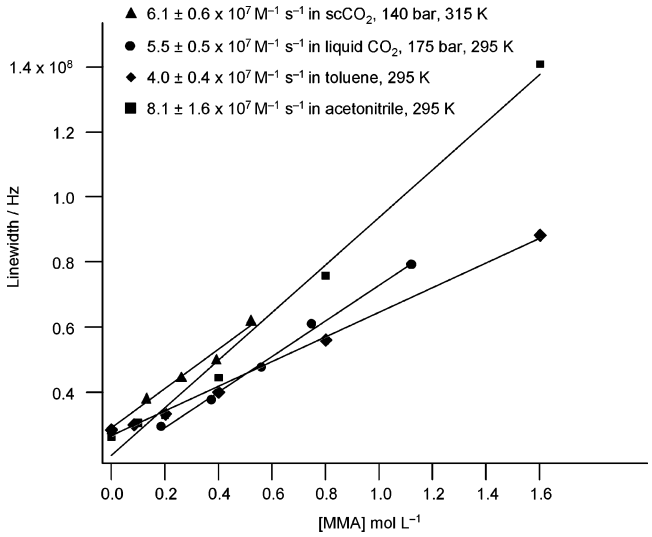

Figure 5. Dependence of the TREPR line width of radical **2b** on MMA concentration during 308 nm photolysis of **2** in liquid CO_2, supercritical CO_2, acetonitrile, and toluene. The rate constants shown at the top represent k_{add} for the addition of radical **2b** to MMA, obtained from the slopes of these plots.

fit the 0.5 μs spectrum in Figure 2B. The simulation is again carried out with only TM polarization (no RPM), and the benzoyl radical is not included. The simulation parameters are listed in the figure caption. The long-range ^{31}P hyperfine doublet of 63.8 G helps to spread all the transitions out, improving the resolution and making the simulation much easier.

The signal due to phosphonyl radical **2b** becomes broader and less intense with increasing delay time. Both the decrease in intensity and the increase in line width are due to chemical reaction. The intensity is function of relaxation, CIDEP generation, and chemical reaction. However, at a constant delay time and microwave power, the line width is affected on this time scale *only* by chemical reaction to produce **2c**. Because it is an isolated transition, we can easily relate its line width directly to this reaction and the MMA concentration. Figure 4 shows normalized high field transitions of radical **2c** as a function of MMA concentration. The signal-to-noise ratio is better for this system due to stronger RPM polarization often observed with radicals having large hyperfine interactions. As expected, there is a pronounced dependence of this line width on the amount of MMA present in the solution.

Figure 5 shows plots of the line width (in Hz) of the high field line of **2b** as a function of MMA concentration in four different solvents. The value of k_{add} is determined directly from the slopes of these plots. Of immediate note is that k_{add} values obtained in liquid and supercritical CO_2 are very similar. Also, the rates in CO_2 are comparable to those observed in acetonitrile, although CO_2 is a much less viscous solvent than either acetonitrile or toluene. Intrinsic barriers to free radical addition reactions to alkenes exist in the form of steric and polar effects and have recently been extensively reviewed.[32] In CO_2 these factors are clearly important, as the rates we have obtained are less than diffusion-controlled. The overall rates measured here are on the high end for addition to alkenes for other initiators but are on the same order of magnitude previously measured for phosphorus-centered radical structures. For this particular radical reacting with MMA, the only literature value for k_{add} available is 1.8×10^8 M^{-1} s^{-1}, obtained in benzene by Mizuta et al.[30] Error limits for those measurements were not reported, but their number is satisfyingly close to ours for all four solvents studied.

Conclusions

We have demonstrated that k_{add} values can be measured in CO_2 using the line width technique of Gatlik et al.[22] The reaction for diphenylphosphonyl oxide radical **2b** to MMA is less than diffusion-controlled and similar to that observed in acetonitrile. For radical **1b** it is possible to state that the addition reaction certainly takes place, but on a slower time scale than for **2b**. More quantitative consideration cannot be attempted for **1b** and **1c** due to spectral overlap and spin relaxation effects. Clearly the phosphorus-centered radical systems from **2** have many advantages for these studies, with large hyperfine coupling constants leading to well-resolved TREPR transitions and strong polarization. Additionally, they show faster reactivity than their carbon-centered analogues. Structural modification studies are currently underway in our laboratory to add to the database of k_{add} values, to investigate polar and steric effects in CO_2, and to further test the generality of this method. We are particularly interested in the role of CO_2 in regard to polar effects because, with no dipole moment but a strong quadrupole moment, significant solvent effects might still be observable depending on the alkene substitution pattern.

Acknowledgment. We are indebted to the National Science Foundation for continued support of our program through Grant CHE-0518300. This work received partial support from the STC Program of the National Science Foundation under Agreement CHE-9876674.

References and Notes

(1) Yamada, B.; Westmoreland, D. G.; Kobatake, S.; Konosu, O. *Prog. Polym. Sci.* **1999**, *24*, 565.
(2) DeSimone, J. M.; Maury, E. E.; Menceloglu, Y. Z.; McClain, J. B.; Romack, T. J.; Combes, J. R. *Science* **1994**, *265*, 356.
(3) *Green Chemistry Using Liquid and Supercritical Carbon Dioxide*; DeSimone, J. M., Tumas, W., Eds.; Oxford University Press: New York, 2003.
(4) Hoggan, E. N.; Flowers, D.; Wang, K.; DeSimone, J. M.; Carbonell, R. G. *Ind. Eng. Chem. Res.* **2004**, *43*, 2113.
(5) Paisner, S. N.; DeSimone, J. M. *Polymers for Microelectronics and Nanoelectronics*; Lin, Q., Pearson, R. A., Hedrick, J. C., Eds.; *ACS Symp. Ser.* **2004**, *874*, 223.

(6) Kennedy, K. A.; Roberts, G. W.; DeSimone, J. M. *Adv. Polym. Sci.*, Okubo, M., Ed.; *Springer* **2005**, *175*, 329−346.
(7) Shaffer, K. A.; Jones, T. A.; Canelas, D. A.; DeSimone, J. M. *Macromolecules* **1996**, *29*, 2704.
(8) Canelas, D. A.; Betts, D. E.; DeSimone, J. M. *Macromolecules* **1996**, *29*, 2818.
(9) Dukes, K. E.; Harbron, E. J.; Forbes, M. D. E.; DeSimone, J. M. *Rev. Sci. Instrum.* **1997**, *68*, 2505.
(10) Wood, C. D.; Yarbrough, J. C.; Roberts, G.; DeSimone, J. M. In *Supercritical Carbon Dioxide in Polymer Reaction Engineering*; Kemmere, M. F., Meyer, T., Eds.; Wiley: Weinheim, Germany, 1989.
(11) Forbes, M. D. E.; Dukes, K. E.; Avdievich, N. I.; Harbron, E. J.; DeSimone, J. M. *J. Phys. Chem. A* **2006**, *110*, 1767.
(12) Avdievich, N. I.; Dukes, K. E.; Forbes, M. D. E.; DeSimone, J. M. *J. Phys. Chem. A* **1997**, *101*, 617.
(13) Sluggett, G. W.; Turro, C.; George, M. W.; Koptyug, I. V.; Turro, N. J. *J. Am. Chem. Soc.* **1995**, *117*, 5148.
(14) Hayashi, H.; Sakaguchi, Y.; Kamachi, M.; Schnabel, W. *J. Phys. Chem.* **1987**, *91*, 3936.
(15) Ananchenko, G. S.; Bagryanskaya, E. G.; Tarasov, V. F.; Sagdeev, R. Z.; Paul, H. *Chem. Phys. Lett.* **1996**, *255*, 267.
(16) Savitsky, A. N.; Galander, M.; Mobius, K. *Chem. Phys. Lett.* **2001**, *340*, 458.
(17) Jent, F.; Paul, H.; Fischer, H. *Chem. Phys. Lett.* **1988**, *146*, 315.
(18) Heberger, K.; Fischer, H. *Int. J. Chem. Kinet.* **1993**, *25*, 249.
(19) Martschke, R.; Farley, R. D.; Fischer, H. *Helv. Chim. Acta* **1997**, *80*, 1363.
(20) Quadir, M. A.; DeSimone, J. M.; van Herk, A. M.; German, A. L. *Macromolecules* **1998**, *31*, 6481.
(21) Kajiwara, A.; Konishi, Y.; Morishima, Y.; Schnabe1, W.; Kuwata, K.; Hamachi, M. *Macromolecules* **1993**, *26*, 1656.
(22) Gatlik, I.; Rzadek, P.; Gescheidt, G.; Rist, G.; Hellrung, B.; Wirz, J.; Dietliker, K.; Hug, G.; Kunz, M.; Wolf, J.-P. *J. Am. Chem. Soc.* **1999**, *121*, 8332.
(23) Harbron, E. J.; Forbes, M. D. E. *Encyclopedia of Chemical Physics and Physical Chemistry*; Institute of Physics Publishing: Philadelphia, 2001; Chapter B1.16, p 1389.
(24) Savitsky, A. N.; Paul, H. *Appl. Magn. Reson.* **1997**, *12*, 449.
(25) Forbes, M. D. E. *Photochem. Photobiol.* **1997**, *65*, 73−81.
(26) Tsentalovich, Y. P.; Forbes, M. D. E. *Mol. Phys.* **2002**, *100*, 1209.
(27) Tsentalovich, Y. P.; Forbes, M. D. E.; Morozova, O. B.; Plotnikov, I. A.; McCaffrey, V. P.; Yurkovskaya, A. V. *J. Phys. Chem. A* **2002**, *106*, 7121.
(28) Makarov, T. N.; Bagryanskaya, E. G.; Paul, H. *Appl. Magn. Reson.* **2004**, *26*, 150.
(29) Karatekin, E.; O'Shaughnessy, B.; Turro, N. J. *Macromolecules* **1998**, *31*, 7992.
(30) Mizuta, Y.; Morishita, N.; Kuwata, K. *Appl. Magn. Reson.* **2000**, *19*, 93.
(31) Makarov, T. N.; Savitsky, A. N.; Mobius, K.; Beckert, D.; Paul, H. *J. Phys. Chem. A* **2005**, *109*, 2254.
(32) Fischer, H.; Radom, L. *Angew. Chem., Int. Ed.* **2001**, *40*, 1340.

MA062438A